# Synthesis and characterization of silk fibroin-bioactive glass hybrid xerogels

Xiaohong Wu[1], Fuhua Yan[*2], Wei Liu[3], Hongbing Zhan[3a] and Wenrong Yang[4]

[1]*School and Hospital of Stomatology, Fujian Medical University, 246 Yangqiao Zhong Road, Fuzhou 350002, China*
[2]*Institute and Hospital of Stomatology, Nanjing University Medical School, 30 Zhongyang Road, Nanjing, Jiangsu, 210008, China.*
[3]*College of Materials Science and Engineering, Fuzhou University, 2 Xueyuan Road, Fuzhou 350108, China*
[4]*School of Life and Environmental Science, Waurn Ponds Campus, Geelong Deakin University, Australia*

**Abstract.** This study aimed to develop a novel bioactive hybrid xerogel consisting of silk fibroin /$SiO_2$-CaO-$P_2O_5$ by sol-gel process at room temperature. Scanning electron microscopy (SEM), FT-IR Spectroscopy, pore measurement, mechanical property testing, in vitro bioactivity test and cytotoxicity assay were performed to characterize the xerogel for bone tissue engineering application. We have found that the xerogel possessed excellent pore structures and mechanical property. Once immersed in a simulated fluid (SBF), the xerogel exhibited profound bioactivity by inducing hydroxyapatite layers on its surfaces. The cell toxicity study also demonstrated that there was little toxic to MC3T3-E1 cells. These results indicate that silk fibroin /$SiO_2$-CaO-$P_2O_5$ hybrid xerogel potentially could be used as a bone tissue engineering material.

**Keywords:** hybrid; xerogel; silk fibroin; $SiO_2$-CaO-$P_2O_5$; bone tissue engineering

## 1. Introduction

The ability to regenerate and self-repair for bone is naturally powerful, but a considerable amount of bone loss or the development of adverse microenvironment could hinder the capacity of spontaneous healing, such as in trauma, infection, tumor resection, bone aging and congenital malformation. Even the current clinical solutions to these problems rely on autologous bone grafting and allografting, but all of them have their own disadvantages. Therefore, the search for new bone repair strategies is imperative. The approaches of bone tissue engineering hold the promise of great therapeutic potential indeed (Grabowski and Cornet 2013, Vallet-Regí *et al.* 2011, Thian and Best 2008). The development of a new class of scaffold materials is a key step in bone tissue engineering.

Bioactive glasses are a group of synthetic, surface-active, composition-dependent and silica-based bioactive materials, composed of $SiO_2$-CaO-$P_2O_5$ chemically bond to tissue without an intervening fibrous layer. There are versatile appealing characteristics for scaffold materials in

---

*Corresponding author, Ph.D., E-mail: fhyan2005@126.com
[a]Ph.D., E-mail: hbzhan@fzu.edu.cn

bone tissue engineering, such as excellent biocompatibility, osteoconductivity, osteoinductivity, and even angiogenic, as well as antibacterial properties (Rahaman *et al*. 2011, Arcos *et al*. 2010, Will *et al*. 2012, Jones *et al*. 2006). In vivo implantation shows that these compositions produce no toxicity, no inflammation, and no foreign-body response (Fu *et al*. 2010, Bi *et al*. 2012). Although bioactive glasses have achieved great application successes in bone repair, the issues such as brittleness and stress shielding produced by elastic modulus mismatch between glasses and bone limit their applications (Jones and Hench 2001). To improve the mechanical property of bioactive glasses, a variety of natural and synthetic biodegradable polymers have been applied to prepare the organic-inorganic composites (Zhai *et al*. 2013, Liu *et al*. 2012, Thiwawong *et al*. 2009). Organic-inorganic hybrid composites constitute a new class of materials with promising properties for constituent components.

Silk fibroin is a fibrous protein polymer isolated from silkworm cocoons (Bombyx mori). It exhibits nonthrombogenic, anti-inflammatory, cell-adhesive, cell-responsive and regenerative properties, providing a remarkable combination of good biocompatibility, slow degradation rate, high strength and toughness compared to other commercial biomaterials such as polylactic acid and collagen, so it is a promising biomaterial used in bone regeneration application (Altman *et al*. 2003, Lovett *et al*. 2007, Mathur and Gupta 2010). However, silk fibroin is not bioactive and not able to form chemical bonds with bone, which limits their use in bone repair. Thus, the composites of inorganic bioactive glasses and organic silk fibroin may offer complementary benefits to each other. Furthermore, nature bone consists of nature polymers, collagen fibers and nanohydroxyapatite (*n*-HA), which is fully integrated at nanoscale, while constituents of traditional composites are mixed only at macroscopic level, which may cause unpredictable dissolution rates and rapidly deteriorating mechanical properties. So, it is of particular interest to synthesize an inorganic-organic hybrid consisting of two constituents at the nanoscale.

In this letter, we synthesized a new class of organic-inorganic hybrid material for a suitable scaffold. Silk fibroin (SF) was hybridized with $SiO_2$-CaO-$P_2O_5$ to form SF/$SiO_2$-CaO-$P_2O_5$ hybrid xerogels by sol-gel process. The bioactivity, mechanical property, pore structure, nanostructures and cell compatibility of the hybrid xerogel were also investigated.


## 2. Materials and methods

### 2.1 Materials

All the reagents were obtained from the Sinopharm Chemical Reagent Company (Shanghai, China) and used without further purification.

### 2.2 Preparation of silk fibroin

Briefly, cocoons from B. mori silkworm were cut and boiled in an aqueous solution of 0.02 M $Na_2CO_3$ for 1 h, then removed and rinsed with distilled water three times. The steps above were repeated until sericin and other impurities were removed from silk fibers absolutely. The purified air-dried silk fibers were then dissolved in $CaCl_2$-$C_2H_5OH$-$H_2O$ solution with a 1:2:8 molar ratio at 75℃ for 30 min. The solution was leached twice to remove insoluble impurities, then dialyzed against distilled water for 1 day using the MWCO 14,000 g/mol dialysis membrane to remove inorganic ions and ethyl alcohol, and the distilled water was changed every 3 h. Then the solution

was dialyzed against 15 wt% PEG (Mw 20 000 g/mol) to condense. The silk fibroin (SF) aqueous solutions had a final concentration of 15~22 wt% and were preserved at 5°C.

## 2.3 Preparation of SF/SiO$_2$-CaO-P$_2$O$_5$ hybrid xerogels

Firstly, tetraethoxysilane (TEOS, 12.3 ml), distilled water (4 ml) and ethanol (6 mL) were mixed at a 1:4:2 ratio. Then trace hydrochloric acid (HCl) was added to adjust pH value to approximately 2 in order to catalyze the hydrolysis of TEOS. After the mixture was stirred for 1 h, calcium chloride (CaCl$_2$, 3.6 g) and triethylphosphate (TEP, 1.2 ml) were introduced as the precursors of calcium and phosphorus, respectively. The amount of CaCl$_2$ and TEP was scaled to obtain a final composition of 60 mol%SiO$_2$-36 mol%CaO-4 mol%P$_2$O$_5$, which is a typical formula of bioglass (Hench 2006). The mixture was stirred until the introduced CaCl$_2$ was dissolved completely. Secondly, SF aqueous solution was added into the system during the hydrolysis reaction of TEOS. The weight of the silk fibroin was calculated to ensure that the mass ratio of organic and inorganic components was 0.2:1. Then, several drops of hydrofluoric acid (HF) were added into the sol under vigorous stirring to accelerate the condensation process and the formation of SiO$_2$ network. When the viscosity of the system increased dramatically, which meant the system was close to the gelatinous point, stirring was stopped. The resultant sol was cast into 24-well polystyrene cell culture plate, sealed, and left to age and dry for a month. All these procedures were handled at room temperature.

## 2.4 Characterization of SF/SiO$_2$-CaO-P$_2$O$_5$ hybrid xerogels

### 2.4.1 Scanning Electon Microscope (SEM)
The morphologies of the surfaces of xerogels were observed by scanning electron microscopy (SEM, Philips-FEI XL30 ESEM-TMP operated at an accelerating voltage of 20 kV). The surfaces were previously sputter-coated with a 20-nm-thick gold layer to avoid surface charging during observation.

### 2.4.2 FT-IR Spectroscopy
Fourier-transform infrared analysis was carried out according to the potassium bromide-pellet technique with a FT-IR spectrometer (Nicolet 5700, Thermo, USA) in the range of 4000-400 cm$^{-1}$ at a spectral resolution of 1 cm$^{-1}$.

### 2.4.3 Thermogravimetric analysis (TGA)
Thermal properties of the samples were examined via a thermogravimetric analyzer (SDT-Q600, TA, USA). Samples were heated in the temperature range from room temperature to 800°C at a scanning rate of 10°C /min under nitrogen atmosphere.

### 2.4.4 Pore measurement
The pore structure was analyzed using a Micromeritics ASAP 2010M Surface Area and Porosimetry analyzer. The nitrogen adsorption–desorption data were recorded at liquid nitrogen temperature (77 K). The samples were previously degassed under vacuum (10-5 mm Hg) for 3 h. The specific surface area was calculated using the Brunauer-Emmett-Teller (BET) analysis. In addition, the pore size distribution curve was determined by the Barrett-Joyner-Halenda (BJH) method.

### *2.4.5 In vitro bioactivity test*

The assessment of in vitro bioactivity was carried out in a simulated body fluid (SBF) (Kokubo and Takadama 2006). A group of xerogels were selected to investigate the correlation between composition and bioactivity. Each specimen was soaked in 30 ml of SBF solution and incubated at 37℃ in a closed polyethylene bottle for up to 14 days. After soaking, the samples were collected, rinsed with distilled water and dried in a desiccator. The samples were observed by SEM and EDX after 0, 1, 7 and 14 days in SBF to determine hydroxyapatite (HAp) formation.

### *2.4.6 Mechanical property testing*

The mechanical property of each sample, especially the elastic modulus, was tested using a nanoindenter (XP, MTS corp, USA) with a Berkovich tip (a triangular pyramid). And the continuous stiffness measurement (CSM) was adopted. For this test, 5 points were selected from the surface of each example. The range of indentation depth was from 1000 nm to 1500 nm.

### *2.4.7 Cytotoxicity assay*

The in vitro cytotoxicity of the xerogels was examined by MTT assays on MC3T3-E1 cells (Shanghai Institutes for Biological Science, Chinese Academy of Sciences). Firstly, the xerogels were sterilized and immersed in $\alpha$-MEM medium at a ratio of 1 g sample to 5 ml medium for 72 h to prepare the leaching liquor. The MC3T3-E1 cells were pre-cultured in $\alpha$-MEM supplemented with 10% fetal bovine serum for 24 hours; then the supernatant was removed and replaced by the leaching liquor (200 $\mu$l for each well). The cells were further cultured in the leach liquor at 37℃ and 5% $CO_2$. After incubation for 24 , 48 and 72 h, the cells were incubated with 20 $\mu$l MTT (5 g/l) for 4 h at 37℃ and 150 $\mu$l DMSO was pipetted to solubilize the formazan product for 20 min at 37℃. The optical density (OD) was determined using a enzyme-labeling instrument at a wavelength of 492 nm. The cell relative growth rate (RGR) was calculated according to the following formula: RGR = (OD sample - OD blank) / (OD negative control - OD blank), and the negative control was the $\alpha$-MEM medium.

## 3. Results and discussion

Mechanical stability, biodegradability, and biocompatibility of biomaterials are essential. Meanwhile, biomaterials should be free from cytotoxins.

As for osteoconductive materials, $SiO_2$-CaO-$P_2O_5$ glass is quite useful in the field of bone tissue engineering. As inorganic materials, it can be easily synthesized through sol-gel technique at room temperature. However, silica xerogels usually are brittle. Based on hybridization with silk fibroin, crack-free and stable hybrid xerogels were fabricated when the ratio of silk fibroin to silica xerogel was 30%. Moreover, the sol-gel process is a useful method to produce homogeneous mixtures of silk fibroin and $SiO_2$-CaO-$P_2O_5$ hybrid xerogels.

The main peaks in the FT-IR spectrum of the xerogels were showed in Fig. 1. The broad and strong overlapped peaks at around 3510 cm$^{-1}$ and middle strong sharp peak at 1620 cm-1 corresponded to the residual water in hybrid xerogels and the stretching vibrations of O-H of Si-OH. The inorganic components of xerogels showed FT-IR peaks in the following regions: 1250-1000 cm$^{-1}$ (stretching vibrations of Si-O-Si), 960-900 cm$^{-1}$ (vibration absorption of Si-OH), and 550-450 cm$^{-1}$ (bending vibrations of Si-O-Si). The presence of residual silanol (Si-OH) is frequently observed in sol-gel derived materials, reflecting incomplete polycondensation (Lee *et al*.
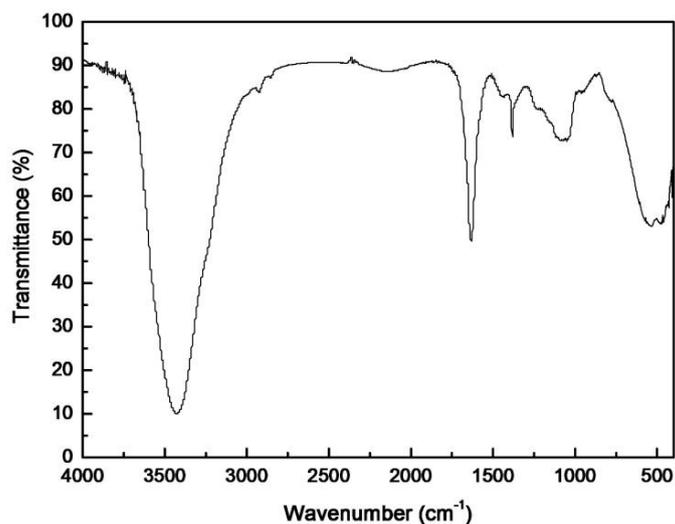
Fig. 1 FT-IR spectrum of SF /$SiO_2$-CaO-$P_2O_5$ xerogel
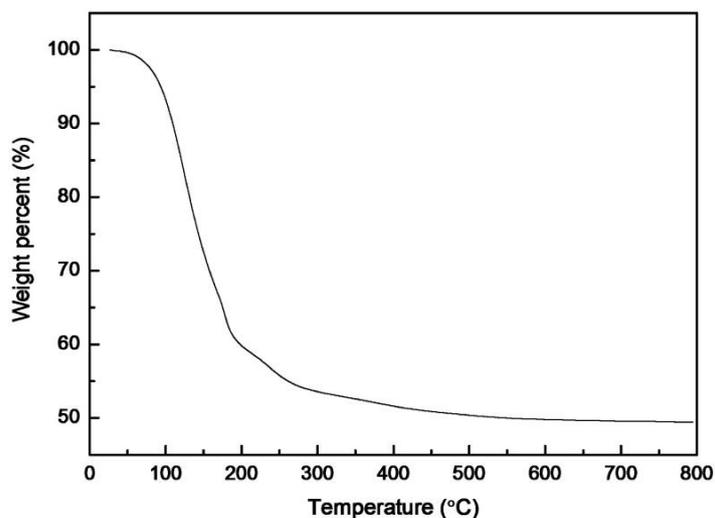


Fig. 2 TG curve of SF /$SiO_2$-CaO-$P_2O_5$ xerogel

2009). C=O stretching vibrations of amido bonds of SF were observed at around 1600 $cm^{-1}$. The sharp peaks at 1380 $cm^{-1}$ were attributed to the stretching vibration of C-H of -$CH_3$ or -$CH_2$. The broad and weak overlapped peaks around 1200-1100 $cm^{-1}$ also corresponded to bending vibrations of C-O of amido bands of SF. These peaks indicated hybridization between organic and inorganic components were successfully obtained. No peaks were observed in the spectrum of the hybrid xerogels, implying that there were no strong covalent bonds between the organic and inorganic components. Furthermore, the interaction of the two phases was moderately weak due to the van der Waals forces, hydrogen or ionic bond between organic and inorganic components.
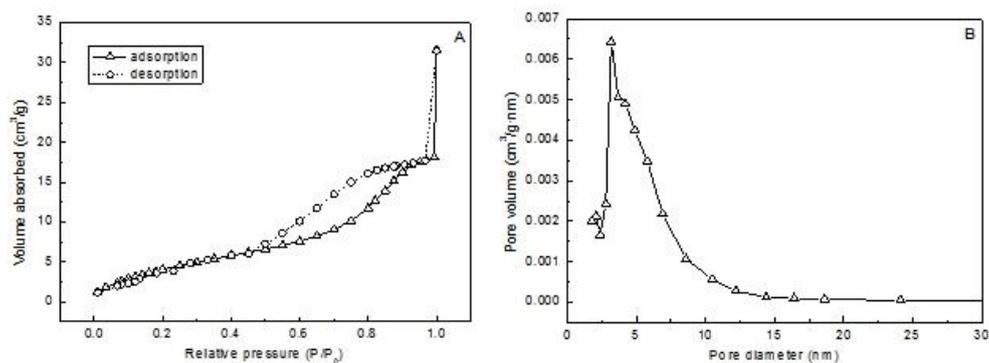
Fig. 3 Nitrogen asdorption-desorption isotherms (A) and pore size distribution from the $N_2$ desorption isotherm (B) of SF /$SiO_2$-CaO-$P_2O_5$ xerogel
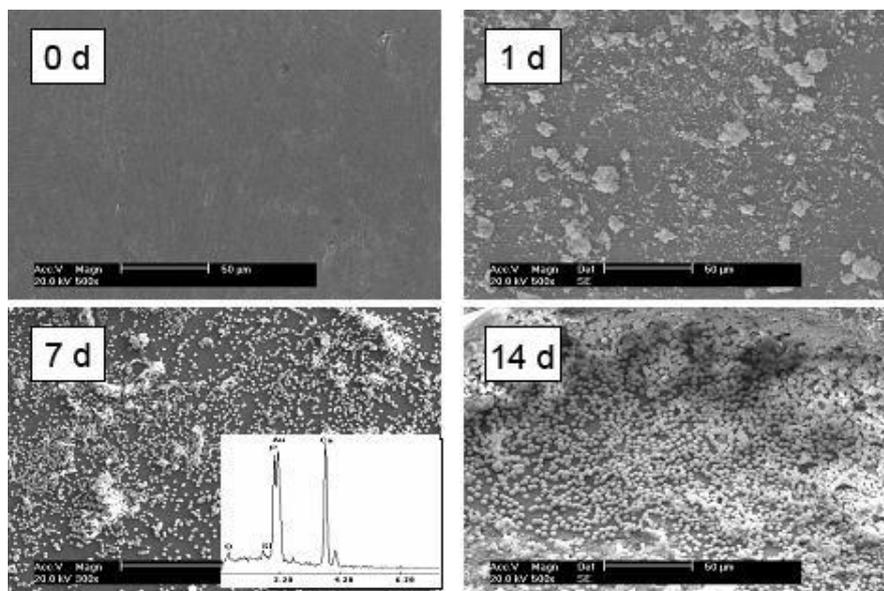


Fig. 4 SEM micrographs of SF /$SiO_2$-CaO-$P_2O_5$ xerogels before and after soaking in SBF for 1, 7 and 14 days. Insets: corresponding energy distribution spectrum of the substance deposited on the sample surface

The TG curve of the xerogels was illustrated in Fig. 2. The rapid weight loss of the sample at 200℃ may be caused by the evaporation of residual solvents and byproducts in the sol-gel process. There was about 15% weight loss around 200-300℃, which was attributed to the decomposition of the organic component SF. When the temperature rose to 800℃, the weight of the xerogels was kept around 50%. Therefore, we could estimate that mass ratio of organic and inorganic components was 0.3:1.

Second, the adsorption-desorption isotherm and corresponding pore size distributions of the xerogels can be seen in Fig. 3. There was a clear hysteresis loop in the adsorption-desorption isothermat high pressure. It indicated the existence of abundant mesopores in the samples. The
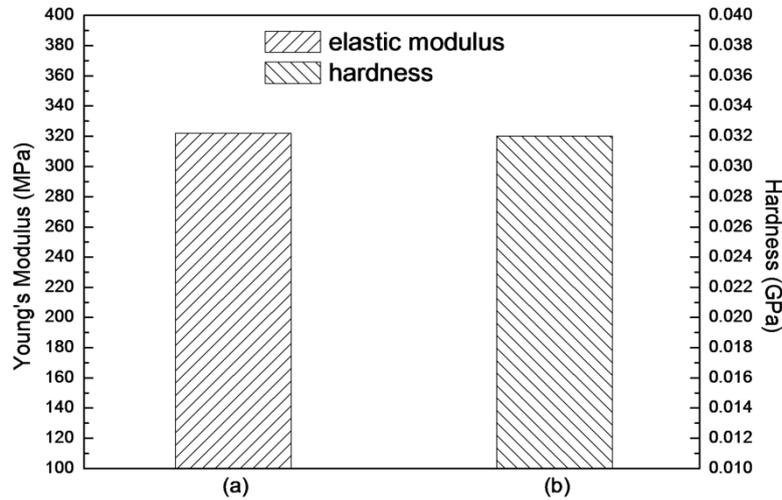
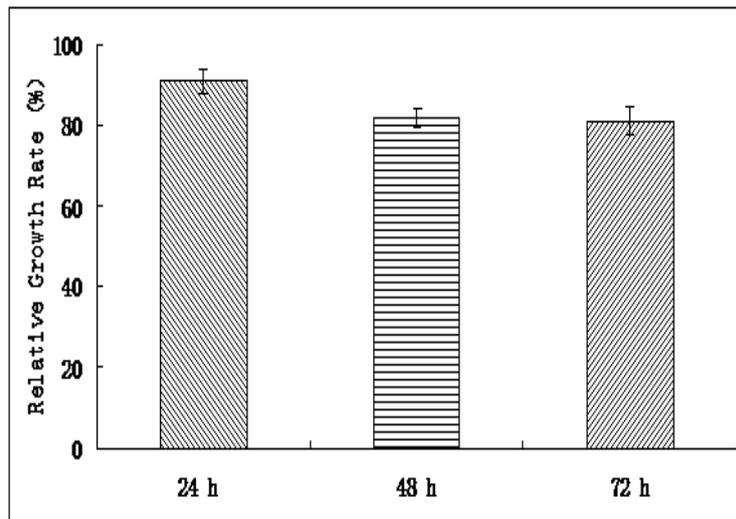Fig. 5 Young's modulus (a) and Hardness (b) of SF /$SiO_2$-CaO-$P_2O_5$ xerogels



Fig. 6 The relative growth rate of MC3T3-E1 cells cultured in the leach liquor of SF /$SiO_2$-CaO-$P_2O_5$ xerogels for 24, 48 and 72 h, respectively. The relative concentration of the leach liquor is 100%

isotherm of the sample possessed a hysteresis loop of particles aggregated into slab-like structure in the interior of the sample, and slit-shaped pores were created. The average pore diameter was 6.4 nm, pore volume was 0.028 $cm^3$/g, and surface area by the BET was 17.6 $m^2$/g. The hysteresis loop was classified as type H3. However the pore size distribution of the sample was broad and we speculated that this resulted from space resistance of SF. Meanwhile, the xerogels could provide adequate space for the inner growth of cells as they degraded. And the degradation products of SF could promote cell proliferation and differentiation as well as formation of new bone and microvessel.

In vitro bioactivity of the xerogels was confirmed by incubating the materials in SBF solution and the change in their surface during incubation. Fig. 4 showed the SEM micrographs of the xerogels before and after immersion in the SBF solutions. The original sample surfaces exhibited a relatively smooth and uniform surface. After immersion for 1 day, a thin mineral layer was formed on the surface of the samples. With the passing of immersion time, the concentration and average sizes of the spherical particles increased. At the 7th days, the shape of particles was near spherical with an average diameter of 2 $\mu$m. After 14 days, particles were agglomerated with more compact structures.

It is a dynamic process for apatite formation on the xerogels surfaces. It has been widely studied that SBF can reproduce the surface changes of certain biomaterials. Through EDS analysis, we found Ca and P on the surface of the sample. The Ca/P peak intensity ratio was 1.44, which was lower than 1.67 of stoichiometric HA, indicating of the presence of a Ca-deficient apatite in the hybrid xerogels (Deng *et al*. 2001). Ca-P deposition was of great interest. The formation of bonelike apatite or Ca/P layer was regarded as an essential factor for biomaterials with bioactivity, which was the ability to form the chemical bond between the bioactive material and living bone tissue. Thus, in vitro bioactivity test supports that the xerogels have a great potential application for repair and regeneration of bone defects.

The mechanical properties of the sample were showed in Fig. 5. The value of elastic modulus was 311 MPa and the hardness value was 0.032 GPa, which were close to (but lower than) those of trabecular bone (Goldstein *et al*. 1983). The xerogels have the ability to resist deformation.

To access the efficacy of the hybrid xerogels, it was essential to test the material cytotoxicity. In our assay, indirect contact method (leaching liquor) was used and the leaching liquor concentration prepared was 100%. As shown in Fig. 6, at three time points, the relative growth rates of cells were all more than 80%, ranging from 94% to 81%, and the relative degrees of in vitro cytotoxicity were all graded 0. Thus, it clearly showed there was little cytotoxic to MC3T3-E1 cells.

## 4. Conclusions

In summary, we demonstrated homogeneous $SF/SiO_2$-$CaO$-$P_2O_5$ hybrid xerogels were successfully prepared at room temperature using sol-gel process. Due to the coherent interaction of the organic and inorganic components, the material exhibited excellent apatite forming ability and excellent mechanical property, as well as pore structure for the ingrowth of cells and new bone tissues. In addition, the xerogels is little cytotoxic to MC3T3-E1 cells. All these results suggested that $SF/SiO_2$-$CaO$-$P_2O_5$ hybrid xerogels have a great potential application in bone tissue engineering.

## Acknowledgments

## References

Altman, G.H., Diaz, F., Jakuba, C., Calabro, T., Horan, R.L., Chen, J., Lu, H., Richmond, J. and Kaplan, D.L. (2003), "Silk-based biomaterials", *Biomater.*, **24**(3), 401-16.

Arcos, D. and Vallet-Regí, M. (2010), "Sol-gel silica-based biomaterials and bone tissue regeneration", *Acta. Biomater.*, **6**(8), 2874-88.

Bi, L., Jung, S., Day, D., Neidig, K., Dusevich, V. Eick, D. and Bonewald, L. (2012), "Evaluation of bone regeneration, angiogenesis, and hydroxyapatite conversion in critical-sized rat calvarial defects implanted with bioactive glass scaffolds", *J. Biomed. Mater. Res. A.*, **100**(12), 3267-75.

Deng, X., Hao, J. and Wang, C. (2001), "Preparation and mechanical properties of nanocomposites of poly (D,L-lactide) with Ca-deficient hydroxyapatite nanocrystals", *Biomater.*, **22**(21), 2867-73.

Fu, Q., Rahaman, M.N., Fu, H. and Liu, X. (2010), "Silicate, borosilicate, and borate bioactive glass scaffolds with controllable degradation rate for bone tissue engineering applications. II. In vitro and in vivo biological evaluation", *J. Biomed. Mater. Res. A.*, **95**(1), 164-71.

Goldstein, S.A., Wilson, D.L., Sonstegard, D.A. and Matthews, L.S. (1983), "The mechanical properties of human tibial trabecular bone as a function of metaphyseal location", *J. Biomech.*, **16**(12), 965-9.

Grabowski, G. and Cornet, C.A. (2013), "Bone graft and bone graft substitutes in spinesurgery: current concepts and controversies", *J. Am. Acad. Orthop. Surg.*, **21**(1), 51-60.

Hench, L.L. (2006), "The story of bioglass", *J. Mater. Sci. Mater. Med.*, **17**(11), 967-78.

Jones, J.R., Ehrenfried, L.M. and Hench, L.L. (2006), "Optimising bioactive glass scaffolds for bone tissue engineering", *Biomater.*, **27**(7), 964-73.

Jones, J.R. and Hench, L.L. (2001), "Biomedical materials for new millennium: perspective on the future", *Mater. Sci. Tech.*, **17**(8), 891-900.

Kokubo, T. and Takadama, H. (2006), "How useful is SBF in predicting in vivo bone bioactivity Biomaterials", *Biomater.*, **27**(15), 2907-15.

Lee, E.J., Shin, D.S., Kim, H.E., Kim, H.W., Koh, Y.H. and Jang, J.H. (2009), "Membrane of hybrid chitosan-silica xerogel for guided bone regeneration", *Biomater.*, **30**(5), 743-50.

Liu, W., Wu, X.H., Zhan, H.B. and Yan, F.H. (2012), "Synethesis of bioactivity poly (ethylene glycol) /SiO2-CaO-P2O5 hybrid xerogels for bone regeneration", *Mater. Sci. Eng., C.*, **32**(4), 707-711.

Lovett, M., Cannizzaro, C., Daheron, L., Messmer, B., Vunjak-Novakovic, G. and Kaplan, D.L. (2007), "Silk fibroin microtubes for blood vessel engineering", *Biomater.*, **28**(35), 5271-9.

Mathur, A.B. and Gupta, V. (2010), "Silk fibroin-derived nanoparticles for biomedical applications", *Nanomedicine*, **5**(5), 807-20.

Rahaman, M.N., Day, D.E., Bal, B.S., Fu, Q., Jung, S.B., Bonewald, L.F. and Tomsia, A.P. (2011), "Bioactive glass in tissue engineering", *Acta. Biomater.*, **7**(6), 2355-73.

Thian, E.S. and Best, S.M. (2008), "Materials viewpoints in bone regenerative medicine: progress and prospects", *Materi. Sci. Tech.*, **24**(9), 1027-1030(4).

Thiwawong, T. And Nukeaw, J. (2009), "Organic/inorganic multilayer hybrid thin films: effect of substrate temperature", *Mater. Res. Innov.*, **13**(3), 165-167.

Vallet-Regí, M, Colilla, M. and González, B. (2011), "Medical applications of organic-inorganic hybrid materials within the field of silica-based bioceramics", *Chem. Soc. Rev.*, **40**(2), 596-607.

Will, J., Gerhardt, L.C. and Boccaccini, A.R. (2012), "Bioactive glass-based scaffolds for bone tissue engineering", *Adv. Biochem. Eng. Biotech.*, **126**, 195-226.

Zhai, H. Quan, Y., Li, L., Liu, X.Y., Xu, X, and Tang, R. (2013), "Spontaneously amplified homochiral organic-inorganic nano-helix complexes via self-proliferation", *Nanoscale*, **5**(7), 3006-12.

*CC*